

**STUDY OF THE EFFECTS OF IONIC LIQUIDS
AS ELECTROLYTE ADDICTIVES FOR REDOX
FLOW BATTERIES**

LIANG XIAOJIAN
(*B.Eng.*, Tsinghua University, China)

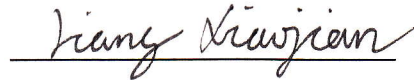
**A THESIS SUBMITTED
FOR THE DEGREE OF MASTER OF SCIENCE
DEPARTMENT OF CHEMISTRY
NATIONAL UNIVERSITY OF SINGAPORE**

2014

DECLARATION

I hereby declare that this thesis is my original work and it has been written by me in its entirety. I have duly acknowledged all the sources of information which have been used in the thesis.

This thesis has also not been submitted for any degree in any university previously.

A handwritten signature in black ink, reading "Liang Xiaojian", written over a horizontal line.

Liang Xiaojian

13 August 2014

ACKNOWLEDGEMENTS

First and foremost, I'd like to show my deepest gratitude to my supervisor, Prof. LI Fong Yau Sam, a respectable, responsible and resourceful professor who has provided me with this precious chance to study in NUS and with valuable guidance. Without his enlightening instruction, impressive kindness and patience, I could not have completed my study. His keen and vigorous academic observation enlightens me not only in this thesis but also in my future study.

I shall extend my thanks to Huang Yan and Lai Linke for all their kindness and help. I would also like to thank all my teachers who have helped me to develop the fundamental and essential academic competence. My sincere appreciation also goes to all the group members.

Last but not least, I'd like to thank all my friends, for their encouragement and support.

TABLE OF CONTENTS

ACKNOWLEDGEMENTS	i
TABLE OF CONTENTS	ii
SUMMARY	iii
LIST OF TABLES	iv
LIST OF FIGURES	v
1. Introduction	1
2 Redox flow batteries	4
2.1 RFBs main features	4
2.2 Pros and cons	6
2.3 RFBs technologies.....	8
2.4 Non-aqueous vanadium RFBs.....	11
3 Ionic liquids as electrolytes	14
4 Experimental	16
4.1 Synthesis of RTILs.....	16
4.1.1 Synthesis of BMImPF ₆	16
4.1.2 Synthesis of BMImBF ₄	16
4.2 Conductivity	17
4.3 Cyclic Voltammetry	17
4.4 Charge-discharge experiments.....	18
5 Results and discussions	19
5.1 Synthesis of ionic liquids.....	19
5.2 Conductivity	19
5.3 Cyclic Voltammetry	20
5.3.1 Voltammetric behavior of V(acac) ₃ in acetonitrile	20
5.3.2 Kinetics of electrode reactions.....	23
5.4 Charge-discharge performance	26
6. Conclusions	29
7. Prospects	30
References	31
Appendix	35

SUMMARY

Many researches on non-aqueous redox flow batteries (RFBs) show that these non-aqueous batteries usually have a wider potential window and higher operating temperature than that of aqueous ones. Relatively low conductivity of solvent is a limitation of good performance. To solve this problem, several ionic liquids including 1-Butyl-3-methylimidazolium hexafluorophosphate (BMImPF₆), 1-Butyl-3-methylimidazolium tetrafluoroborate (BMImBF₄) were synthesized and introduced as electrolyte additive into all vanadium non-aqueous RFB system. Results from cyclic voltammetry indicate that BMImPF₆ could be expected to improve the performance of all vanadium RFB system while BMImBF₄ was not suitable for the system due to the low stability window.

The diffusion coefficients for solutions containing different concentrations of BMImPF₆ and BMImBF₄ were calculated from CVs at varying scan rates. Results show the diffusion coefficient increased as the concentration of ionic liquids increased. For a solution containing 0.5 mol L⁻¹ BMImPF₆ the diffusion coefficient can be 4.94~8.00 × 10⁻⁶ for V(II)/V(III) redox couple and 6.30~10.20 × 10⁻⁶ for V(III)/V(IV) redox couple.

The charge-discharge characteristics for the system were evaluated in a self-designed cell. Three plateaus with respect to reactions between V(V)/V(IV) and V(II)/V(III), V(IV)/V(III) and V(II)/V(III), along with reactions related to byproducts of the VO(acac)₂ formation were observed at 2.5 V, 1.8V and 0.9 V, respectively. A coulombic efficiency near 50% was obtained at 50% state of charge for an electrolyte containing 0.5 mol L⁻¹ BMImPF₆.

LIST OF TABLES

Table 1 Design and operating feature of main energy storage systems

Table 2 Best performance and typical figures of electrochemical energy storage systems

Table 3 Elemental analysis results of ionic liquids

Table 4 Conductivity of different concentration of ionic liquid in acetonitrile

Table 5 Diffusion coefficient of $V(acac)_3/BMIImPF_6$ in acetonitrile

Table 6 Diffusion coefficient of $V(acac)_3/BMIImBF_4$ in acetonitrile

LIST OF FIGURES

Fig. 1 Diagram of a RFB energy storing system

Fig. 2 Cyclic voltammograms recorded at 0.5 V s^{-1} at a glassy carbon electrode in $0.01 \text{ M V}(\text{acac})_3$ and 0.5 M BMImPF_6 in acetonitrile and $0.01 \text{ M V}(\text{acac})_3$ without ionic liquids in acetonitrile.

Fig. 3 Cyclic voltammogram recorded at 0.5 V s^{-1} at a glassy carbon electrode in $0.01 \text{ M V}(\text{acac})_3$ and 0.5 M BMImBF_4 in acetonitrile.

Fig. 4 Cyclic voltammograms at a glassy carbon electrode in $0.01 \text{ M V}(\text{acac})_3$ with 0.5 M BMImPF_6 in acetonitrile. The scan rate was varied from 0.01 to 0.5 V s^{-1} .

Fig. 5 Full discharge of a full-charged system containing $0.01 \text{ M V}(\text{acac})_3$ with 0.5 M BMImPF_6 in acetonitrile at a constant current of 0.5 mA .

Fig. 6 Charge–discharge curves for $0.01 \text{ M V}(\text{acac})_3$ with 0.5 M BMImPF_6 in acetonitrile. The charge current was 4.5 mA and the discharge current was 0.5 mA .

1. Introduction

Nowadays the rapid development of industrial societies has relied on the exploitation of low-cost fossil energy. Large quantities of fossil fuel can only be formed over a long time, but they have been burned in a relatively short time, with substantial environment impact. According to World Energy Outlook in 2011, the electric energy demand exceeds 20×10^3 TW h per year and is still growing at a rate of about 3% per year [1, 2]. This huge amount of electric energy comes mainly from fossil fuel, which occupies two third of total energy production. As the total amount of fossil fuel is limited and the formation of fossil fuel will take a long time, the choice of energy source appears to be unsustainable. To meet the growing demand for energy as well as to mitigate the environmental problems that caused by the usage of conventional energy sources, many countries, particularly large industrialized countries pay more attention to the environmental friendly and renewable energy sources, such as wind, solar and other type of sources.

Renewable sources, except hydropower, currently provide 4% of electricity production mainly from wind and solar energy. This number is estimated to grow by more than 25% by the year of 2030 [3]. These renewable sources are intermittent because they generate electrical power according to the time and climate availability, which are different from conventional power sources. Thus, the integration of primary energy sources with renewable sources requires more attention in the

design, control and management of the electric grid [4]. The grid should be stable and in good performance when the intermittent energy comes in. To meet this demand, energy storage, one of compensating measures, is imported. The energy storage system can store energy if the energy production has surplus and use the surplus to cope with higher demand in others [5-7]. This kind of system will be essential parts of smart grids which are expected to spread in the near future.

There are several energy storage systems that can provide such performance, including pumped hydro energy storage (PHES) and compressed air energy storage (CAES) for the large scale, and thermal energy storage for relatively small scale. The design and operating feature of main energy storage systems are shown in Table 1. Among all energy storage systems, PHES, CAES and thermal energy storage (TES) are suitable for long-time-scale grid energy storage. Though flywheel energy storage (FES), superconducting magnetic energy storage (SMES) and electric double layer capacitor (EDLC) have very fast response time, the cost of these systems is very high.

Table 1 Design and operating feature of main energy storage systems [8]

Technology	Scalability	Flexibility	Environmental impact	Safeness issue
PHES	Good	Low	High	High
CAES	Low	Low	High	High
TES	Low	Low	Mild	Mild
FES	High	Good	Low	Mild
SMES	Good	Low	Low	Low
EDLC	Low	Low	Low	Mild
ECES	Good	Good	Low	Low

Several surveys show that electrochemical energy storage systems (ECES) are the solution of choice for assisting intermittent renewable energy generators, with short- to long-time-scale energy storage, because of their site versatility, modularity that allows wide scalability, ease of operation, and static structure [9, 10]. They are expected to have wide implementation in the coming years as distributed storage systems and substantial funds have been already allocated for their scientific and technological development. Forecasts indicate a growth to 150 GW of installed power, corresponding to 10,000 times more than present capacity [11]. Best performance and typical figures of electrochemical energy storage systems are shown in Table 2.

Table 2 Best performance and typical figures of electrochemical energy storage systems [8]

Technology	Top power [MW]	Top energy [MW h]	Energy density [W h kg ⁻¹]	Response time	Round-trip efficiency	Cycle life × 10 ³	Capital cost [k\$ kW ⁻¹]
Advanced lead-acid	10-40	1-10	25-50	ms	75-85%	3	4.6
Sodium-sulfur	34	10	150-120	s	85-90%	4.3-6	3.5
Sodium-nickel-chlorine*	1	6	95-120	s	85%	3-4	3.5
Lithium-ion	16	20	100-200	ms	95%	4-8	3-4
Electrolyzer/fuel cell	1	>10	800-1300	ms	35-45%	50	17
Redox flow battery	2-100	6-120	10-50	ms	85%	>13	3.2

* Data courtesy of FIAMM S.p.A—Zebra-Sonick (Italy)

2 Redox flow batteries

Among all the electrochemical energy storage systems, redox flow batteries represent one of the most recent technologies and a highly promising choice for stationary energy storage [12, 13]. A redox flow battery is actually a sort of fuel cell and is similar to a polymer electrolyte membrane fuel cell. The most appealing features of RFBs are: scalability and flexibility, independent sizing of power and energy, high round-trip efficiency, high DOD, long durability, fast responsiveness, and reduced environmental impact [14], making them an ideal technology for assisting electricity generation from renewable sources.

2.1 RFBs main features

The RFBs are electrochemical energy conversion devices, which store energy by exploiting redox processes of species in solution. Generally speaking, a RFB consists of several parts: cell, tanks, pumps and accessories, as shown in Fig. 1. Redox fuel cell is the place where redox processes happen and it is the most important part of one RFB; The species, usually called redox couple, are stored in external tanks in fluid form and pumped into the RFB when redox processes happen; The accessories, including converter, connect RFBs to the grid so that this system can store electricity from other sources and generate electricity when needed.

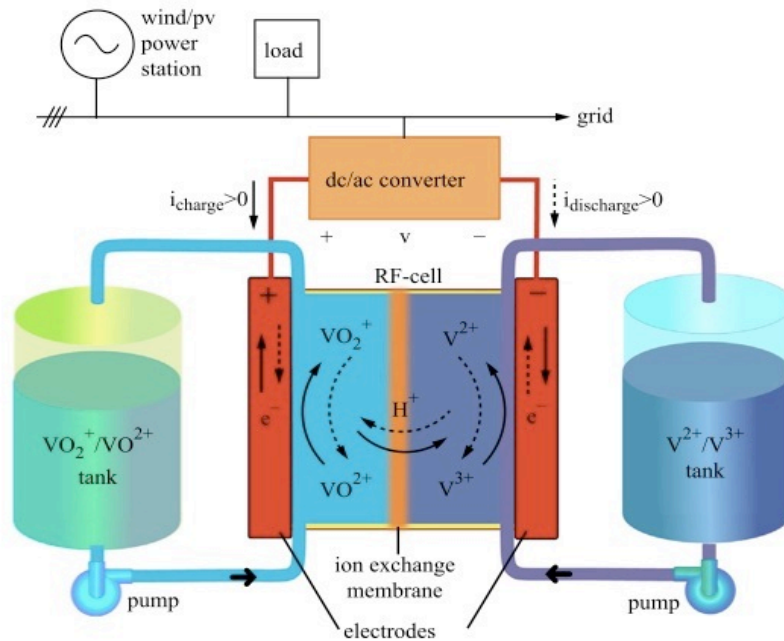


Fig.1 Diagram of a RFB energy storing system

The principle behind a RFB cell is a couple of electrochemical reduction and oxidation reactions occurring in two electrolytes containing metal ions [15]. When charging or discharging happens, the reduction half-reaction at one electrode extracts electrons and ions from one electrolyte, while the oxidation half-reaction at the other electrode absorb the electrons and recombines them with redox species in the other electrolyte. The electrons can't move from one electrolyte to the other inside the cell because the membrane that separate two electrolytes is impermeable to electrons. Thus, electrons are forced to move through external circuit that providing electric energy exchange. In the meantime, ions can move through membranes to keep electronic balance of the whole solution in redox fuel cell. Both half-cells are connected to external tanks, extending the volume of electrolyte solutions available for energy storage.

2.2 Pros and cons

Compared with other electrochemical storage technologies, in RFBs, power conversion is separated from energy storage. This allows for independent power and energy sizing, making the scalability very good. RFBs can exceed most ECES technologies by one order of magnitude only by using larger tanks to store electrolytes.

The electrochemical heart of RFBs is the membrane electrode assembly, a sandwich structure consisting of two catalyzed electrodes with an interposed polymeric membrane. To allow electrolyte flow toward the electro-active sites, the electrodes are required to have a porous structure that can be obtained with carbon based materials such as carbon felt, carbon fiber or carbon nanotubes. This feature can achieve a compromise between good electrode permeability and high electrode active area [14].

The most important advantage RFBs have is that the reactions happen in both half-cells are completely reversible, which enables the same cell to operate as converter of electricity into chemical energy and vice-versa. RFBs operate by changing the metal ion valence without consuming ion metals so that RFBs usually have a longer cycle service life. This operation can also lead to an easy management in storing and handling the electrolytes, because the electrolytes can be kept in two low-cost tanks and only two pumps are needed for circulating the electrolytes between the tanks and the cell electrodes.

Besides, there are other advantages in RFBs. Cell temperature of RFBs is easily controlled by regulating the electrolyte flow, which allows the RFBs to operate the cells in the optimal condition; RFBs are capable of rapid response, which allows them to span from power quality to energy management services; Moreover, rapid refueling by solution exchange is possible, and furthermore low maintenance is required in RFBs.

The most important disadvantage that RFBs have is that the power density and energy density are low compared with other technologies, making them unsuitable for mobile applications at present. Accordingly, cell active areas and membranes are quite large, increasing the dimensions of the battery and causing high transverse gradients of the solutions flowing toward the sites of electrochemical activity inside the electrodes. Consequently, this reduces the average current density and nominal current with respect to the maximum theoretical values, achievable with uniform maximum current density [8].

Other disadvantages include: the conductive electrolytes are prone to shunt currents, which produce additional losses and affect electric efficiency; RFBs are required to operate around room temperature to keep the solutions in the liquid phase, which calls for heat/temperature control by means of specifically designed systems. However, on the whole, RFBs energy storage system is an excellent technology.

2.3 RFBs technologies.

The vanadium (V) redox couple was first mentioned in a 1933 patent by P. A. Pissoort, in France (Patent 754 065-1933) and a patent on a titanium chloride flow cell was registered by Walter Kango in Germany in 1954 [16].

Early systematic studies were undertaken in the 1970s within NASA's space programs by Thaller [17-19], starting with Fe/Ti electrolytes [20]. These research programs included the investigation of other redox couples including Fe/Cr [21].

The vanadium idea was revived in 1978 in Italy by A. Pelligri and P. M. Spaziante (GB Patent 2030349-1978), but without significant development. The first known successful demonstration and commercial development of redox flow batteries employing vanadium in each half cell (VRB, Vanadium/vanadium Redox Battery) was carried out at the University of New South Wells (UNSW), AU, by Skyllas-Kazacos, who registered a patented in 1986 (AU Patent 575247-1986) [22-24]. At that time the interest in vanadium in Australia was enhanced by new mining programs aimed at catapulting the country to a leading position among vanadium producers worldwide.

The VRB system is the only technology that has reached effective commercial fruition [25]. It uses vanadium/vanadium dissolved in aqueous sulfuric acid (~5 M). An advantage is that by using the same metal ions in both electrolytes, the electrodes and membrane are not

cross-contaminated and the cell capacity does not decrease with time, allowing for a longer lifespan.

However, some differences in the metal ion charge oxidations at the two electrodes must exist, so that vanadium IV–V (tetravalent–pentavalent) is used on one side and vanadium II–III (bivalent–trivalent) on the other, thereby exploiting the ability of this element to exist in solution in four different oxidation states.

During charging at the positive electrode tetravalent vanadium within VO^{2+} ions is oxidized to pentavalent vanadium within VO_2^+ ions, while at the negative electrode trivalent ions V^{3+} are reduced to bivalent ions V^{2+} . The hydrogen ions 2H^+ move through the membrane to maintain the electrical neutrality of the electrolytes. The standard OCV of a VRB cell is $E^0=1.26$ V at 25 °C, but in fact real cells exhibit $E^0=1.4$ V due to the correcting Nernst's factors.

VRBs exhibit a current density in the order of 50–80 mA/cm² and correspondingly a power density barely reaching 0.1 W cm⁻², which is much lower than that of equivalent PEMFCs. Stored energy density does not exceed 25–35 W h L⁻¹. Active cell areas in the order of 6000 cm² and over are needed for managing currents of some hundreds of amperes in a single cell.

There are several advantages of VRB that can be summarized here: (i) by employing the same element in both half-cells and utilizing four different oxidation states of vanadium in solution, in comparison to the Fe/Cr system, the VRFB eliminates the problem of cross contamination

by diffusion of different redox ions across the membrane. Even if solution crossover occurs, the electrolytes can be regenerated by mixing and then electrolysis without complicated chemical treatment;

(ii) it does not require a catalyst for each electrode reaction and the relatively fast kinetics of the vanadium redox couples allow high charge and voltage efficiencies to be obtained, the overall energy efficiency from an initial 71% up to 90% has been reported with a 1 kW VRFB stack;

(iii) there is an extremely low rate of gas evolution during the charge rates associated with rapid charging cycles;

(iv) it can be overcharged and deeply discharged, within the limits of the capacity of the electrolytes, as well as being cycled from any state of charge or discharge, without permanent damage to the cell or electrolytes;

(v) a reusable electrolyte leads to a long cycle life and reduces cost of the system. These advantages and its flexibility make the VRFB a promising technology for large-scale storage of renewable energy [26].

However, VRB system still faces some challenges for practical applications. A major one is low energy density. Compared to other batteries for energy storage, a 25~30 W h kg⁻¹ is quite low. This is mainly due to the limited concentration of vanadium species in H₂SO₄. Although some efforts have been done to improve the solubility and the stability of vanadium species, low energy density still remains a major challenge. Besides, the cost and the possible degradation of the ion-exchange membrane and the positive electrode are other challenges for VRB system.

2.4 Non-aqueous vanadium RFBs

Aqueous electrolytes are normally used in most RFB systems. Due to the water content in the aqueous electrolyte, cell voltage is often limited by the electrochemical window of water electrolysis, which is 1.229 V. The operating temperature is lower than 100 °C due to the evaporation of water. The possibility of using organic non-aqueous electrolytes in RFB have been recently evaluated as, in principle, they were considered to have a wider potential window, larger temperature range and higher power density than their aqueous counterparts.

Among all non-aqueous systems, Vanadium acetylacetonate ($V(acac)_3$) as a single metal for non- aqueous RFBs has been predominantly studied [27-30]. The $V(acac)_3$ redox flow system employing acetonitrile and $TEABF_4$ was developed to be an H-type cell assembled with graphite electrodes and an anion exchange membrane [28]. There are three oxidation states for the redox reaction in this system, and the electrolyte containing $V(acac)_3$ initially exists in both compartments (the anolyte and catholyte compartments). During discharge, $V(acac)_3$ is oxidized to $[V(acac)_3]^+$ at the positive electrode (anode) and is reduced to $[V(acac)_3]^-$ at the negative electrode (cathode); thus, the decline of coulombic efficiency caused by the cross-contamination of electrolytes is improved by using the same electrolyte in both compartments. The evaluated cell potential is approximately 2.18 V, and coulombic efficiencies of around 50% are observed at a 50% state of oxidation for the electrolyte. Since two redox couples revert to the same state of

oxidation in the discharge mode, a higher cell potential and lower cross-over are obtained in the non-aqueous $V(\text{acac})_3$ redox system. In the same redox system, Shinkle et al. also used an anion exchange membrane to separate the anolyte and catholyte [30]. They investigated the water and oxygen effects on the performance of the system. The reduction of $V(\text{acac})_3$ is repressed on carbon, and the solvent and support electrolyte might have been degraded by oxygen. In addition, the kinetics of the negative $V(\text{acac})_3$ redox couple is impeded via the formation of vanadyl acetylacetonate by water. Thus, prior to cell assembly, the membrane is immersed in the electrolyte for a long time to remove any environmental water or oxygen in most experiments. Furthermore, the effect of the supporting electrolyte for the $V(\text{acac})_3$ redox system was recently investigated in an H-type cell assembled with an anion exchange membrane by Zhang et. al. [29]. They synthesized and offered tetrabutylammonium hexafluorophosphate (TEAPF_6) and 1-ethyl-3-methyl imidazolium hexafluorophosphate (EMIPF_6) as the supporting electrolytes for improving the performance of the $V(\text{acac})_3$ redox system. The cell potentials for the TEAPF_6 and EMIPF_6 systems are 2.3 V and 2.4 V, respectively. These cell potential results in this report is higher than that of $V(\text{acac})_3$ system when using TEABF_4 as the supporting electrolyte (2.18 V). In the other study, three electrode materials - i.e. glassy carbon, platinum, and gold - were explored for their application in non-aqueous $V(\text{acac})_3$ RFBs in the same electrolyte configuration as

used in previous cases [27]. The exchange-current densities measured on glassy carbon, platinum, and gold electrodes for the $V(acac)_3$ reduction reaction were 1.3, 3.8, and 8.4 $A\ m^{-2}$, respectively.

3 Ionic liquids as electrolytes

As mentioned above, several kinds of supporting electrolytes, i.e. TEAPF₆, EMIPF₆ and so on, are used in non-aqueous systems to improve the performance of RFB systems. This kinds of supporting electrolytes are called ionic liquid due to their unique properties. Classical solutions of electrolytes are obtained by dissolution of salts in molecular solvents. Such systems consist of solvated ions, their charged or neutral combinations and solvent molecules. On the other hand, a salt may be melted down, or in other words 'liquified', by providing to the system a heat to counterbalance the salt lattice energy. Such a system, called molten salts or ionic liquid (IL), consists of ions and their combinations and is free of any molecular solvent [32]. The term "ionic liquid" is often extended to salts having a melting point below 100 °C. In such a case a significant amount of heat must be provided to keep the salt in the liquid state, and IL cannot be handled as a classical electrolyte solution.

A specific kind of IL, called room temperature ionic liquid or RTIL, has been picked out due to the practical aspects of their maintenance or handling and a lot of researches have been done to study the application in electrochemistry. RTILs are salts having a low melting point are liquid at room temperature, this makes it possible to apply RTILs into RFBs to improve the performance.

Although some researches have been done to study the physical and chemical properties of RTILs in electrochemistry, there are few

research about the application of different RTILs in RFBs. Most articles focus on three RTILs, i.e. TEAPF₆, EMIPF₆ and TEABF₄. So the objectives of this project is to apply different ionic liquids into non-aqueous redox flow batteries as electrolyte additive and study their electrochemical properties of different ionic liquids in non-aqueous redox flow batteries.

4 Experimental

To apply different RTILs in non-aqueous RFBs, several RTILs, including 1-butyl-3-methylimidazolium hexafluorophosphate (BMImPF₆), 1-butyl-3-methylimidazolium tetrafluoroborate (BMImBF₄) were firstly synthesized. Then, cyclic voltammetry was done to acquire the CV curve, and then calculate the diffusion coefficient. Due to the strong corrosive effect of vanadium acetylacetonate (V(acac)₃), a cell made of PTFE was designed to complete the charge-discharge test.

4.1 Synthesis of RTILs

4.1.1 Synthesis of BMImPF₆

1-Methylimidazol 0.1 mol, 1-bromobutane 0.1 mol and potassium salt of hexafluorophosphate 0.1 mol were stirred in a three-necked flask with a reflux condenser at 80 °C for 3.5 h. Then, 10 mL deionized water was added and bi-phase of water/ionic liquids formed, the immiscible ionic liquids BMImPF₆ layer was separated from the water phase. BMImPF₆ layer was washed with sufficient fresh deionized water until the water phase didn't react with AgNO₃ aq. and then the layer was washed with 15 mL diethyl ether for three times. BMImPF₆ was then dried in vacuum at 120 °C for 2 h after it was separated [33]. The compound was analyzed by ¹H NMR.

4.1.2 Synthesis of BMImBF₄

1-Methylimidazol 0.1 mol, 1-bromobutane 0.1 mol and sodium salt of tetrafluoroborate 0.1 mol were stirred in a three-necked flask with a reflux condenser at 80 °C for 3.5 h. Then, the mixture was diluted with

50 mL of acetonitrile. After elimination of the precipitated salts that consist of KBr or NaBr, the filtrate was filtered through a pad of celite to remove the residual halide salt. Then, rotary evaporation was done to afford the ionic liquids [33]. The compound was analyzed by ^1H NMR.

4.2 Conductivity

The conductivity of ionic liquids with different concentration in acetonitrile were measured by Hash HQ14d Portable Conductivity Meter with IntelliCAL™ CDC401 Standard Conductivity Probe.

4.3 Cyclic Voltammetry

Cyclic Voltammetry was performed by a three-electrode system using an ivium A09008 electrochemical station. A glassy carbon electrode (CH Instruments, Inc. USA) with a surface area of 0.07 cm^2 was used as the working electrode. The working electrode was firstly polished in suspension of aluminum powder with diameter of 1 micrometer and then polished in suspension of aluminum powder with diameter of 0.3 micrometer. Then, the electrode was ultrasonically cleaned and rinsed thoroughly with distilled water. A non-aqueous silver/silver ion electrode (CH Instruments, Inc. USA) was used as a quasi-reference electrode. 0.1 mol L^{-1} tetrabutylammonium perchlorate (TBAP) with 0.01 mol L^{-1} AgNO_3 in acetonitrile was filled in reference electrode. A platinum wire electrode (CH Instruments, Inc. USA) was used as counter electrode. 0.01 mol L^{-1} vanadium acetylacetonate was used as active species. $\text{V}(\text{acac})_3$ was dissolved in acetonitrile and 10 mL of the solution was added in a glass bottle. Then, different concentration of ionic liquids

were added in and dissolved. Prior to the experiments, all solutions were purged with research grade nitrogen for at least 15 minutes.

4.4 Charge-discharge experiments

A cell made of PTFE was designed for the charge-discharge experiments. Each compartment contained 10.5 mL of electrolytic solution with a Teflon magnetic stirrer. The electrolytes were separated by an AMI-7001 anion-exchange membrane (Membrane International Inc., US). The membranes were activated by dipping in 5% NaCl solution at 25 °C for 24 h. Prior to the experiment, the membranes were pre-conditioned by soaking them in the test solution for 1 h. Two 30 mm × Φ 6 mm graphite electrodes and a Neware BTS-5V3A battery tester were employed in the charge-discharge experiments. Constant current conditions were used, with the charge current at 4.5 mA and the discharge current at 0.5 mA.

5 Results and discussions

5.1 Synthesis of ionic liquids

^1H NMR was done to analyze the RTILs. For BMImPF₆, the chemical shifts of ^1H NMR (300 MHz, acetone-d₆) are: 8.85 (s, 1H, CH), 7.69 (s, 1H, CH), 7.63 (s, 1H, CH), 4.32 (t, 2H, CH₂), 4.00 (s, 3H, CH₃), 1.91 (m, 2H, CH₂), 1.37 (m, 2H, CH₂), 0.93 (t, 3H, CH₃); For BMImBF₄, the chemical shifts of ^1H NMR (300 MHz, acetone-d₆) are: 8.85 (s, 1H, CH), 7.69 (s, 1H, CH), 7.63 (s, 1H, CH), 4.32 (t, 2H, CH₂), 4.00 (s, 3H, CH₃), 1.91 (m, 2H, CH₂), 1.37 (m, 2H, CH₂), 0.93 (t, 3H, CH₃). The spectral data tally with the structure.

The elemental analysis was also performed on these ionic liquids and the results are shown in Table 3. The data indicate that there are no faults, especially halide salts in the RTILs.

Table 3 Elemental analysis results of ionic liquids

Ionic liquid	C wt%	H wt%	N wt%	Br
BMImPF ₆	33.45	5.14	9.74	Not detected
BMImBF ₄	33.93	5.10	9.30	Not detected

5.2 Conductivity

The conductivity data of BMImPF₆ and BMImBF₄ with different concentration ranging from 0.1 to 0.5 mol L⁻¹ are shown in Table 4. When BMImPF₆ were added into acetonitrile, the conductivity increased from 4 $\mu\text{S cm}^{-1}$ to about 10 mS cm^{-1} , this indicates that ionic liquids as supporting electrolyte can significantly increase the conductivity of the solvent. Within a certain concentration of ionic

liquids, when concentration increased, conductivity of both solution increased, as ions are separated by solvent neutral molecules. Note that conductivity of non-aqueous solutions are significantly lower than aqueous solutions, even with the presence of ionic liquids.

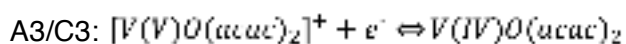
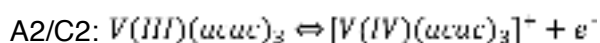
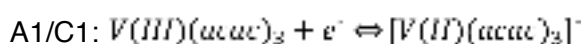
Table 4 Conductivity of different concentration of ionic liquid in acetonitrile (mS cm^{-1})

	0.1M	0.2M	0.3M	0.4M	0.5M
BMImPF ₆	11.45	19.47	25.7	31.1	35.5
BMImBF ₄	7.34	12.27	16.22	19.38	22.2

5.3 Cyclic Voltammetry

5.3.1 Voltammetric behavior of V(acac)₃ in acetonitrile

The black line in Fig. 2 shows a cyclic voltammogram for 0.01 mol L⁻¹ V(acac)₃ with 0.5 mol L⁻¹ BMImPF₆ in acetonitrile at a scan rate of 0.5 V s⁻¹. For comparison, a background CV for 0.01 mol L⁻¹ V(acac)₃ without ionic liquid in acetonitrile at the same scan rate is shown as dotted line. The stability potential window for this system was from -2.5 V to 1.0 V vs. Ag/Ag⁺, or approximately 3.5 V wide. Three redox couples were observed within the stability window. These couples have been attributed to following reactions [34]:



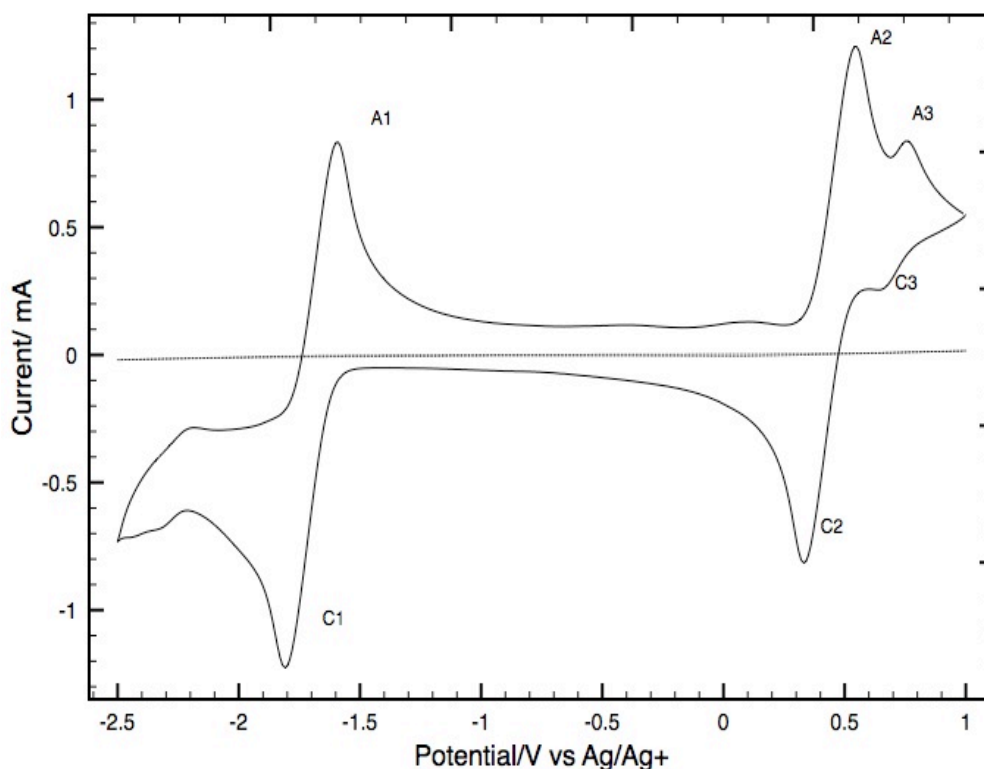
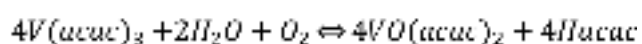


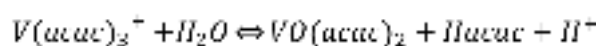
Fig. 2 Cyclic voltammograms recorded at 0.5 V s^{-1} at a glassy carbon electrode in 0.01 M V(acac)_3 and 0.5 M BMImPF_6 in acetonitrile (—) and 0.01 M V(acac)_3 without ionic liquids in acetonitrile (- - -). Measurements were taken at room temperature.

The appearance of the third couple was due to the degradation of V(acac)_3 . V(acac)_3 will react with oxygen and water vapor in ambient environment to form VO(acac)_2 according to the reaction below [35]:



Besides these three main reactions, there are several side reactions that may appear. The side reactions are mostly between redox species and water or/and oxygen in the ambient environment. The presence of dissolved molecular oxygen brings about a step to a very negative limiting current at low voltages, as well as manifesting a reversible redox couple near $-1.25 \text{ V vs. Ag/Ag}^+$ and several irregular oxidation features over the range between 0.0 and $0.5 \text{ V vs. Ag/Ag}^+$; The presence of dissolved water can react with V(acac)_3 to form vanadyl

acetylacetonate ($\text{VO}(\text{acac})_2$) according to the reaction as followed, which is an irreversible step and significantly affects the negative vanadium couple, manifesting irreversible peaks near -1.0 and 0.25 V vs. Ag/Ag^+ :



From the potentials of each half reaction, it can be concluded that a useful cell potential for this system would be 2.2 V. This cell potential is approximately 60% higher than the potential for aqueous vanadium RFBs (1.26 V under standard conditions).

Fig. 3 shows the cyclic voltammogram for 0.01 mol L^{-1} $\text{V}(\text{acac})_3$ with 0.5 mol L^{-1} BMImBF_4 in acetonitrile at a scan rate of 0.5 V s^{-1} . The stability window for this system is -2.5 V to 0 V vs. Ag/Ag^+ , or approximately 2.5 V wide. There is only one redox couple observed in the stability window, which indicates that this system can't be used as both catholyte and anolyte.

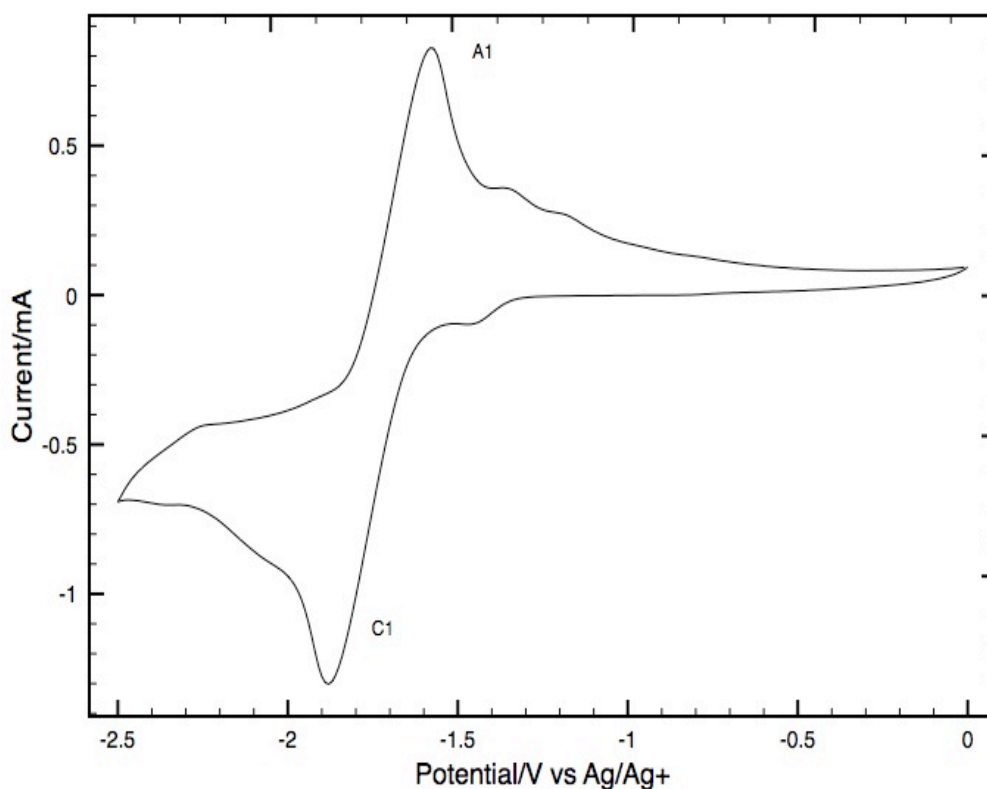


Fig. 3 Cyclic voltammogram recorded at 0.5 V s^{-1} at a glassy carbon electrode in $0.01 \text{ M V}(\text{acac})_3$ and 0.5 M BMImBF_4 in acetonitrile (—). Measurements were taken at room temperature.

5.3.2 Kinetics of electrode reactions

Fig.4 shows a series of CVs at varying scan rates ($0.05, 0.07, 0.1, 0.2, 0.3, 0.4$ and 0.5 V s^{-1}) for electrolytic solutions containing $0.01 \text{ mol L}^{-1} \text{ V}(\text{acac})_3$ with $0.5 \text{ mol L}^{-1} \text{ BMImPF}_6$ in acetonitrile. For the V(II)/V(III) couple, the peak separation increased from 130 to 270 mV as the scan rate increased from 0.01 to 0.5 V s^{-1} . Similarly, for the V(III)/V(IV) redox couple, the peak separation increased from 120 to 270 mV as the scan rate increased. For both redox couples, the ratios of anodic peak currents to cathodic peak currents were near unity, which indicates that the kinetics of electrode reactions are quasi-reversible.

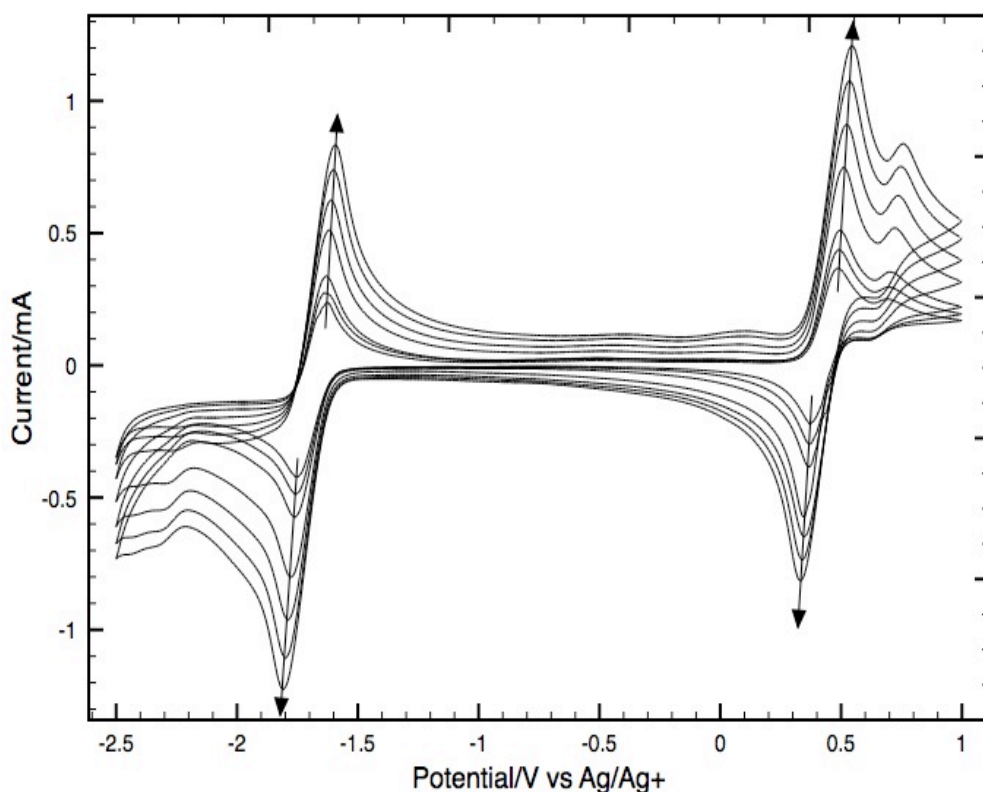


Fig. 4 Cyclic voltammograms at a glassy carbon electrode in 0.01 M V(acac)₃ with 0.5 M BMImPF₆ in acetonitrile. The scan rate was varied from 0.01 to 0.5 V s⁻¹. Measurements were taken at room temperature.

For a quasi-reversible redox couple, the diffusion coefficient, D_0 , is between that for a reversible redox couple and for an irreversible redox couple. For a reversible redox couple, the peak current, i_p , is given by [36]:

$$i_p = 2.69 \times 10^5 n^{3/2} A C D_0^{1/2} v^{1/2}$$

For an irreversible redox couple, the peak current is given by [36]:

$$i_p = 2.99 \times 10^5 n^{3/2} \alpha^{1/2} A C D_0^{1/2} v^{1/2}$$

where n is the number of electrons transferred in the electrode reaction ($n=1$), A is the electrode area ($A=0.07 \text{ cm}^2$), C is the bulk concentration of primary reactant ($C=0.01 \text{ mol L}^{-1}$), α is the transfer coefficient ($\alpha=0.5$). D_0 is the diffusion coefficient of primary reactant and v is the

scan rate. A plot of i_p vs. $v^{1/2}$ yields a straight line with a slope proportional to D_0 . As both redox couples appear to show quasi-reversible kinetics, the value for the diffusion coefficient of $V(acac)_3$ is expected to be in the range of these two values calculated by two equations. The diffusion coefficients for $V(acac)_3$ in $BMIImPF_6$ with different concentration ranging from 0.1 to 0.5 mol L⁻¹ are shown in Table 5.

Table 5 Diffusion coefficient of $V(acac)_3/BMIImPF_6$ in acetonitrile

Concentration (mol L ⁻¹)	V(II)/V(III)		V(III)/V(IV)	
	reversible	irreversible	reversible	irreversible
0.1	2.94×10^{-6}	5.00×10^{-6}	4.30×10^{-6}	6.02×10^{-6}
0.2	3.59×10^{-6}	5.81×10^{-6}	4.79×10^{-6}	6.51×10^{-6}
0.3	4.28×10^{-6}	6.93×10^{-6}	5.64×10^{-6}	7.89×10^{-6}
0.4	4.65×10^{-6}	7.55×10^{-6}	6.00×10^{-6}	8.83×10^{-6}
0.5	4.94×10^{-6}	8.00×10^{-6}	6.30×10^{-6}	1.02×10^{-5}

Similarly, the diffusion coefficients for $V(acac)_3$ in $BMIImBF_4$ with different concentration ranging from 0.1 to 0.5 mol L⁻¹ are shown in Table 6.

Table 6 Diffusion coefficient of $V(acac)_3/BMIImBF_4$ in acetonitrile

Concentration (mol L ⁻¹)	V(II)/V(III)	
	reversible	irreversible
0.1	2.90×10^{-6}	4.69×10^{-6}
0.2	3.60×10^{-6}	5.83×10^{-6}
0.3	3.77×10^{-6}	6.11×10^{-6}
0.4	4.55×10^{-6}	7.38×10^{-6}
0.5	5.05×10^{-6}	8.58×10^{-6}

For both ionic liquids in acetonitrile, as the concentration increased, the diffusion coefficient increased. This may be due to the increase of conductivity of both solutions. For BMImPF₆, the diffusion coefficient archived a value of $4.94\sim 8.00 \times 10^{-6}$ for V(II)/V(III) redox couple and a value of $6.30\sim 10.20 \times 10^{-6}$ for V(III)/V(IV) redox couple, which is higher than that of TEABF₄ with same concentration in acetonitrile [28].

5.4 Charge-discharge performance

Charge-discharge characteristics for a cell containing 0.01 mol L⁻¹ V(acac)₃ and 0.5 mol L⁻¹ BMImPF₆ in acetonitrile were evaluated. A full discharge graph of a full-charged system is illustrated in Fig. 5. There are three discharge plateaus that appear at 2.5 V, 1.8 V and 0.9 V, respectively. The plateau which appears at 2.5 V may be attributed to the reactions between V(V)/V(IV) on anode and V(II)/V(III) on cathode. The potential difference between this two redox couples in CV is about 2.5 V; Another plateau which appears at 1.8 V is due to the reactions between V(IV)/V(III) on anode and V(II)/V(III) on cathode, which has a potential difference of 2.2 V in CV; The last plateau that appears at 0.9 V may have been associated with byproducts of the VO(acac)₂ formation reactions [35]. An over potential of about 400~500 mV was observed with respect to reaction between V(IV) to V(III) and V(II) to V(III).

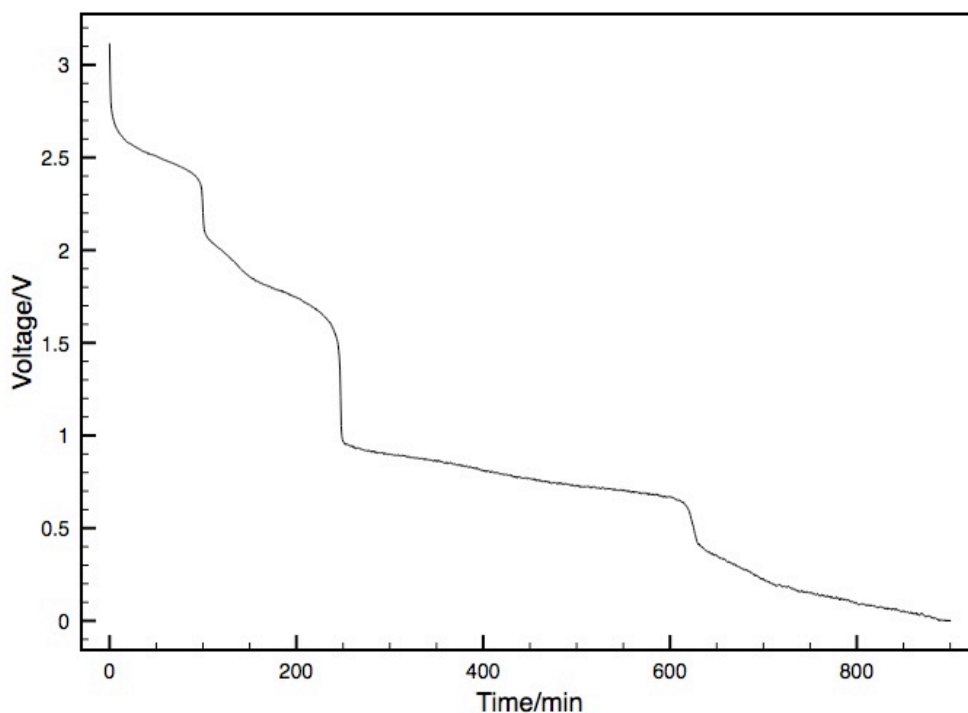


Fig. 5 Full discharge of a full-charged system containing 0.01M $V(acac)_3$ with 0.5M $BMImpF_6$ in acetonitrile at a constant current of 0.5 mA.

A charge-discharge test at 50% state of charge on system containing 0.1 mol L^{-1} $V(acac)_3$ with 0.5 mol L^{-1} $BMImpF_6$ in acetonitrile at a constant charging current of 4.5 mA and discharging current of 0.5 mA is illustrated in Fig. 6. The charge voltages were as high as about 4 V in the first several cycles and achieved about 4.2 V at seventh cycle, while the discharge voltage began at about 2 V. This large ohmic voltage drop may be due to the low conductivity of the electrolyte and the relatively large distance between the two electrodes. A coulombic efficiency of about 50% was achieved for this system. The loss of coulombic efficiency may be attributed to the side reactions and/or the crossover of the active species through the anion-exchange membrane, which causes the loss of active species in the system.

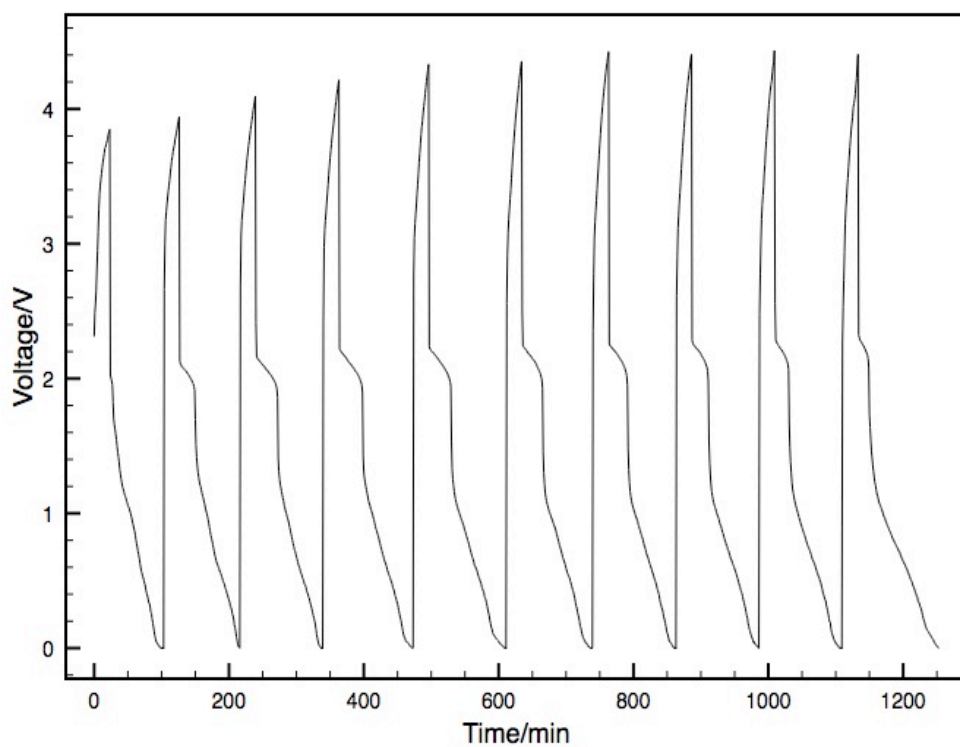


Fig. 6 Charge–discharge curves for 0.01 M $V(acac)_3$ with 0.5 M $BMIImPF_6$ in acetonitrile. The charge current was 4.5 mA and the discharge current was 0.5 mA. Measurements were taken at room temperature.

6. Conclusions

Two ionic liquids were synthesized and introduced as electrolyte additives into the all vanadium RFB system. Results from cyclic voltammetry indicate that BMImPF₆ could be expected to improve the performance of all vanadium RFB system while BMImBF₄ was not quite suitable for the system due to the low stability window.

The diffusion coefficients for solutions containing different concentrations of BMImPF₆ and BMImBF₄ were calculated from CVs at the varying scan rates. Results show the diffusion coefficient increased as the concentration of ionic liquids increased. For a solution containing 0.5 mol L⁻¹ BMImPF₆ the diffusion coefficient can be 4.94~8.00 × 10⁻⁶ for V(II)/V(III) redox couple and 6.30~10.20 × 10⁻⁶ for V(III)/V(IV) redox couple, which are higher than that of TEABF₄ with same concentration in all vanadium RFB system [28].

The charge-discharge characteristics for the system were evaluated in a self-designed cell. Three plateaus with respect to reactions between V(V)/V(IV) and V(II)/V(III), V(IV)/V(III) and V(II)/V(III), along with reactions related to byproducts of the VO(acac)₂ formation were observed at 2.5 V, 1.8 V and 0.9 V, respectively. A coulombic efficiency near 50% was obtained at 50% state of charge for an electrolyte containing 0.5 mol L⁻¹ BMImPF₆.

7. Prospects

The diffusion coefficient of BMImPF₆ and BMImBF₄, as well as charge-discharge performance had been studied in this project. However, the improvement is not as great as we expected. More ionic liquids with higher conductivity should be introduced into the all vanadium RFB system to find out if there is a greater improvement on the performance, especially coulombic efficiency.

To limit the degradation of active species, the cell should be of a good seal. As vanadium is a strong corrosive material when half reactions happen, the cell should also be able to withstand strong corrosion. In our early experiment, a cell made of acrylic glass failed to survive under such condition and was heavily damaged during experiment within 24h. The cell made of PTFE was also slightly damaged during charge-discharge test; however, it didn't quite affect the experiment. A better design of the cell should be of a great help to improve the performance.

More works can also be done on anion exchange membrane or electrodes. There are still problems about crossover and loss of active species that caused by the lack of commercially anion exchange membranes. However, this is outside the scope of this study.

References

- [1]World Energy Outlook 2011, International Energy Agency. 2011.
<http://www.worldenergyoutlook.org>
- [2]Annual Energy Outlook 2012 Early Release Overview, U.S. Energy Information Administration. 2012. <<http://www.eia.gov/forecasts/aeo/er>>
- [3]European Commission. Proposal for a COUNCIL DECISION establishing the Specific Programme Implementing Horizon 2020-The Framework Programme for Research and Innovation (2014–2020), COM(2011) 811 final, 2011/0402 (CNS).
- [4]E. Coster, J. Myrzik, B. Kruimer, W. Kling. Integration issues of distributed generation in distribution grids. Proceedings of the IEEE. 2011; 99(1): 28–39.
- [5]J. Kondoh, I. Ishii, H. Yamaguchi, A. Murata, K. Otani, K. Sakuta, N. Higuchi, S. Sekine, M. Kamimoto. Electrical energy storage systems for energy networks. Energy Conversion and Management. 2000; 41(17): 1863–74.
- [6]B. P. Roberts, C. Sandberg. The role of energy storage in development of smart grids. Proceedings of the IEEE. 2011; 99(6): 1139–44.
- [7]T. Hennessy. DOE energy storage systems research program, annual peer review. Washington DC; 3 November 2006.
- [8]A. Piergiorgio, G. Massimo, M. Federico. Redox flow batteries for the storage of renewable energy: A review. Renewable and Sustainable Energy Reviews. 2014; 29:325–335
- [9]B. Dunn, H. Kamath, J. Tarascon. Electrical energy storage for the grid: a battery of choices. Science. 2011; 334: 928–35.

- [10]Z. Yang, J. Zhang, M. C. Kintner-Meyer, X. Lu, D. Choi, J. P. Lemmon, J. Liu. Electrochemical Energy Storage for Green Grid. *Chemical Reviews*. 2011; 111: 3577–613.
- [11]L. Ren, Y. Tang, J. Shi, J. Dou, S. Zhou, T. Jin. Techno-economic evaluation of hybrid energy storage technologies for a solar-wind generation system. *Physica C: Superconductivity*. 2013; 484: 272–5.
- [12]T. Shigematsu. Redox flow batteries for energy storage. *SEI Technical Review*. 2011; 73: 4–13.
- [13]C. Ponce de León, A. Frías-Ferrer, J. González-García, D. A. Szánto, F. C. Walsh. Redox flow cells for energy conversions. *Journal of Power Sources*. 2006; 160: 716–32
- [14]Z. Weber, M. M. Mench, J. P. Meyers, P. N. Ross, J. T. Gostick, Q. Liu. Redox flow batteries: a review. *Journal of Applied Electrochemistry*. 2011; 41: 1137–64
- [15]M. Skyllas-Kazacos, M. H. Chakrabarti, S. A. Hajimolana, F. S. Mjalli, M. Saleem. Progress in flow battery research and development. *Journal of the Electrochemical Society*. 2011; 158(8): R55–R79
- [16]M. Bartolozzi. Development of redox flow batteries. A historical bibliography. *Journal of Power Sources*. 1989; 27: 219–234
- [17]L. H. Thaller. Electrically rechargeable redox flow cells NASA TM X-71540, Lewis Research Centre, 1-5, 1974
- [18]L. H. Thaller. Performance mapping studies in redox flow cells NASA TM X-82707, Lewis Research Centre, 1-6, 1974
- [19]J. Giner, L. Swette, K. Cahill. Screening of redox couples and electrode materials NASA CR-134705, Lewis Research Centre, 1-107, 1976

- [20]M. Reid, R. Gahn. Factors affecting the open-circuit voltage and electrode kinetics of some Iron/Titanium redox Flow Cells NASA-TM-X-73669, Lewis Research Centre, 1-11, 1977
- [21]L. H. Thaller. Redox flow cell energy storage system NASA TM-79143, Lewis Research Centre, 1-8, 1979
- [22]B. Sun, M. Skyllas-Kazacos. A Study of the V(II)/V(III) redox couple for redox cell application. *Journal of Power Sources*. 1985; 15: 179–90
- [23]B. Sun, M. Rychik, M. Skyllas-Kazacos. Investigation of the V(V)/V(IV) system for use in the positive half-cell of a redox battery. *Journal of Power Sources*. 1985; 16: 85–95
- [24]M. Rychik, M. Skyllas-Kazacos. Characteristics of a new all vanadium redox flow battery. *Journal of Power Sources*. 1988; 22: 59–67
- [25]C. Menictas, M. Skyllas-Kazacos. Performance of vanadium-oxygen redox fuel cell. *Journal of Applied Electrochemistry*. 2011; 41: 1223–32
- [26]P. Leung, X. H. Li, Carlos Ponce de León, L. Berlouis, C. T. John Lowa, F. C. Walsh. Progress in redox flow batteries, remaining challenges and their applications in energy storage. *RSC Advances*. 2012; 2: 10125–10156
- [27]A. A. Shinkle, A. E. S. Sleightholme, L. T. Thompson, C. W. Monroe. *Journal of Applied Electrochemistry*. 2011; 41: 1191–1199.
- [28]Q. H. Liu, A. E. S. Sleightholme, A. A. Shinkle, Y. D. Li, L. T. Thompson. *Electrochemistry Communications*. 2009; 11: 2312–2315.
- [29]D. Zhang, Q. Liu, X. Shi, Y. Li. *Journal of Power Sources*. 2012; 203: 201–205.
- [30]A. A. Shinkle, A. E. S. Sleightholme, L. D. Griffith, L. T. Thompson, C. W. Monroe. *Journal of Power Sources*. 2012; 206: 490–496

- [31]S. H. Shin, S. H. Yun, S. H. Moon. A review of current developments in non-aqueous redox flow batteries: characterization of their membranes for design perspective. *RSC Advances*. 2013; 3: 9095-9116
- [32]M. Galin´ski, A. Lewandowski, I. Stepniak. Ionic liquids as electrolytes. *Electrochimica Acta*. 2006; 51: 5567–5580
- [33]D. Fang, J. Cheng, K. Gong, Q. R. Shi, X. L. Zhou, Z. L. Liu. A green and novel procedure for the preparation of ionic liquid. *Journal of Fluorine Chemistry*. 2008; 129: 108–111
- [34]M. A. Nawi, T. L. Riechel. Electrochemical studies of vanadium (III) and vanadium (IV) acetylacetonate complexes in dimethylsulfoxide. *Inorganic Chemistry*. 1981; 20 (7): 1974–1978
- [35]A. A. Shinkle, A. E. S. Sleightholme, L. D. Griffith, L. T. Thompson, C. W. Monroe. Degradation mechanisms in the non-aqueous vanadium acetylacetonate redox flow battery. *Journal of Power Sources*. 2012; 206: 490–496
- [36]A.J. Bard, L.R. Faulkner, *Electrochemical Methods – Fundamentals and Applications*, second ed., Wiley, 2001

Appendix

The blue print of cell for charge-discharge test (Unit: mm)

